Stochastic resonance in biological nonlinear evolution models

Jörn Dunkel,[1,*] Stefan Hilbert,[1] Lutz Schimansky-Geier,[1] and Peter Hänggi[2]
[1]*Institut für Physik, Humboldt-Universität zu Berlin, Newtonstraße 15, D-12489 Berlin, Germany*
[2]*Institut für Physik, Universität Augsburg, Universitätsstrasse 1, D-86135 Augsburg, Germany*
(Received 30 October 2003; revised manuscript received 2 February 2004; published 28 May 2004)

We investigate stochastic resonance in the nonlinear, one-dimensional Fisher-Eigen model (FEM), which represents an archetypal model for biological evolution based on a global coupling scheme. In doing so we consider different periodically driven fitness functions which govern the evolution of a biological phenotype population. For the case of a simple harmonic fitness function we are able to derive the exact analytic solution for the asymptotic probability density. A distinct feature of this solution is a phase lag between the driving signal and the linear response of the system. Furthermore, for more complex systems a general perturbation theory (linear response approximation) is put forward. Using the latter approach, we investigate stochastic resonance in terms of the spectral amplification measure for a quadratic, a quartic single-peaked, and for a bistable fitness function. Our analytical results are also compared with those of detailed numerical simulations. Our findings vindicate that stochastic resonance does occur in these nonlinear, globally coupled biological systems.

DOI: 10.1103/PhysRevE.69.056118 PACS number(s): 02.50.Ey, 05.40.−a, 87.23.−n

I. INTRODUCTION

Noise-induced order phenomena continue to attract ever growing interest among the practitioners of statistical and biological physics, and also among experimental researchers who put these diverse concepts to use. In particular, the fact that an optimally chosen dose of noise can boost the response and enhance the ability of information and particle transduction in nonlinear systems is known under the labels of stochastic resonance [1–4] and Brownian motors [5–8]. These concepts start to play an increasingly important role in biological systems [1,3,5,7] where noise can assist the functional behavior in a beneficial manner. In this spirit, we study within this work the generalized one-dimensional *Fisher-Eigen model* (FEM), representing a standard model of biological evolution with an intrinsic *global selection coupling* [9–13]. In the Fisher-Eigen model a species (e.g., some biological population) is described by a time-dependent, normalized probability density $p(x,t) \geqslant 0$ which is defined on a set G. In the biological context, G is interpreted as the phenotype space. Furthermore, it is assumed that there exists a fitness function $F(x,t)$ probing each phenotype $x \in G$ at time t. The evolutionary equation of this model is the nonlinear *Fisher-Eigen equation* (FEE)

$$\frac{\partial p}{\partial t} = [F - \overline{F}(t)]p + D\nabla^2 p, \tag{1}$$

where $\overline{F}(t)$ denotes the time-dependent, average fitness function

$$\overline{F}(t) = \int_G dx F(x,t)p(x,t) \tag{2}$$

of the population, and $D > 0$ is a mutation or diffusion parameter. Apparently, the FEE (1) is a nonlocal and nonlinear partial differential equation (PDE): in contrast to the usual Fokker-Planck equation it *does not* have the form of a continuity equation but instead involves explicitly the "potential"

$$U(x,t) = -F(x,t)$$

rather than its "force" $\nabla F(x,t)$. Note also that the Fisher-Eigen equation distinctly differs from nonlinear effective Fokker-Planck equations with self-consistent nonlinear drift and diffusion coefficients [14–20]. The conservation (normalization) of the overall population follows from Eq. (1) by an integration over x using appropriate boundary conditions.

The effect of the selective first term on the right-hand side (rhs) of Eq. (1) is clear: it causes an increase of the local population, if the local fitness value $F(x,t)$ is bigger than the ensemble average $\overline{F}(t)$ and to a decrease, otherwise. Nonlocality or global coupling means that the change of the local population in the phenotype interval $[x, x+dx]$ between time t and $t+dt$ is also influenced by those parts of the overall population, which are located far away from x. In this sense, models with nonlocal selection are based on the assumption that the corresponding system includes long-range information transfer mechanisms, which is of course typical of biological systems.

Besides *selection*, the second fundamental feature of biological evolution is *mutation*. In the FEE mutation processes are realized by diffusion in the phenotype space G. Of course, in real biological systems G is a high-dimensional space. However, for the aim of our studies it is appropriate to confine the discussion to one dimension; more exactly, we set $G = \mathbb{R}$ throughout this paper.

Our main objective is the investigation of the Fisher-Eigen model for fitness functions of the type

$$F(x,t) = F_0(x) + x\, S \sin(\omega t), \quad S > 0, x \in \mathbb{R}. \tag{3}$$

This goal is closely related in spirit to the problems of *sto-*

*Electronic address: dunkel@physik.hu-berlin.de

chastic synchronization [21,22] and *stochastic resonance* [1–3,23]. In particular, we shall be interested in two fundamental situations: (i) The time-independent part $F_0(x)$ of the fitness function possesses only a single maximum, as it is the case for a harmonic fitness, i.e.,

$$F_0(x) = -\frac{a}{2}x^2, \quad a > 0; \tag{4}$$

and (ii) we also consider examples of the type

$$F_0(x) = \frac{a}{2}x^2 - \frac{b}{4}x^4, \quad a,b > 0, x \in \mathbb{R} \tag{5}$$

possessing two equivalent states of maximal fitness at $x_\pm = \pm\sqrt{a/b}$.

In the biological context, the meaning of a bistable fitness function of the type (ii) can be illustrated as follows. Consider a biological species that is characterized by a certain phenotypical feature. Then each value $x \in G$ decodes a possible realization of this feature. Now assume that there coexist two optimal states x_- and x_+, corresponding to two equivalent maxima $F_0(x_\pm)$. That is, those members of the species who are described by $x = x_\pm$ have the highest survival probability. If changes in the environment occur on time scales much larger than the reproduction time of a generation of individuals, then the fitness function can be taken as approximately time independent, $F(x,t) = F_0(x)$.

On the other hand, realistic biological systems are often subject to periodic or at least quasiperiodic environmental changes (e.g., seasons or glacial epochs), which should also be reflected by the fitness function. A simple way to include such effects is realized in Eq. (3), where the time-independent fitness function $F_0(x)$ is superimposed by a time-periodic signal. If, as in the above examples (4) and (5), the function $F_0(x)$ is even, $F_0(-x) = F_0(x)$, then this symmetry is broken in the related time-dependent fitness function (3). In particular, for the bistable example (5) this means that, depending on the external periodic signal, now either states $x \approx x_-$ or states $x \approx x_+$ correspond to maximal fitness values.

For the case (i) of a quadratic fitness function an exact analytic solution of the FEE can be found by using an appropriate ansatz. By virtue of this exact solution one is, in principle, able to compare with results found for driven Fokker-Planck models, characterized by a *local coupling* [1,23,24]. The harmonic case corresponding to Eq. (4) will be extensively discussed in Sec. II.

In principle, one can formulate the generic solution of the FEE (1) in terms of a series expansion. This will be shown in Sec. III. For more complicated examples, such as Eq. (5), it becomes impossible to find closed solutions. Hence approximative linear response techniques must be applied. The corresponding methods are developed in Sec. IV A. In Sec. IV B 1 it is shown that these techniques yield the exact solution for the harmonic case (4). Subsequently, in Secs. IV B 2 and V the perturbation theory is also applied to a single-peaked and a double-peaked quartic fitness function. In these examples stochastic resonance effects can be observed, which in contrast are distinctly absent for harmonic fitness functions. In general, we always test the analytical linear response results by comparing with numerical results based on numerically integrated solutions of the FEE (1). A summary of the main results will be given in Sec. VI.

Before starting out, we still want to mention that evolution processes described by the Fisher-Eigen equation (1) can also serve as role models for evolutionary algorithms of numerical optimization. In this latter context the Fisher-Eigen model is, for obvious reasons, also referred to as "Darwin strategy." A detailed discussion of this aspect including applications to optimization problems (e.g., optimization of road networks) can be found in Refs. [25–28].

II. THE CASE OF A QUADRATIC FITNESS FUNCTION

Note that, for the sake of simplicity, we shall assume throughout this paper that all variables are already given in scaled, dimensionless form. Our objective is to identify whether stochastic resonance does, in principle, also emerge in nonlinear, globally coupled ensembles of the type of the Fisher-Eigen models.

A. Solution via an ansatz

In this part we consider the quadratic fitness function (4)

$$F_0(x) = -\frac{a}{2}x^2, \quad a > 0,$$

which depicts a single peak at $x = 0$. Including a time-periodic perturbation $F_0(x)$ is generalized to read

$$F(x,t) = -\frac{a}{2}x^2 + xS\,\sin(\omega t). \tag{6}$$

The time-independent problem with $S = 0$ was studied earlier in Refs. [29,30]. Here we concentrate on the more interesting case $S \neq 0$. In order to solve the corresponding FEE (1) with the quadratic "potential" $U(x,t) = -F(x,t)$, we attempt the Gaussian ansatz

$$p(x,t) = \frac{1}{Z(t)}\exp\{B[F_0(x) + A\,x\,\sin(\omega t + \phi)]\}, \tag{7}$$

where A, B, and ϕ denote free parameters, which must be determined by inserting this ansatz into the FEE (1). By integration the time-dependent normalization constant $Z(t)$ is found as

$$Z(t) = \sqrt{\frac{2\pi}{aB}}\exp\left[\frac{A^2B}{2a}\sin^2(\omega t + \phi)\right]. \tag{8}$$

Thus, we can rewrite Eq. (7) as

$$p(x,t) = \sqrt{\frac{a\,B}{2\pi}}\exp\left\{-\frac{B}{2a}[a\,x - A\,\sin(\omega t + \phi)]^2\right\}, \tag{9}$$

simply representing a Gaussian with an oscillating mean value. Note that due to the special shape of ansatz (9) we confine ourselves to time-periodic solutions, which are automatically asymptotically stable. By inserting Eq. (9) into the FEE and subsequently ordering the resulting equation with respect to powers of x, one is led to the equation

$$g_0 + g_1\, x + g_2\, x^2 \equiv 0, \tag{10}$$

with coefficients

$$g_0 = a(2aD\, B^2 - 1) - A\, B\, \sin(\omega t + \phi)[2A\, B\omega\, \cos(\omega t + \phi) - 2S\, \sin(\omega t) + A(1 + 2aD\, B^2)\sin(\omega t + \phi)], \tag{11a}$$

$$g_1 = 2aB[A\, B\, \omega\, \cos(\omega t + \phi) - S\, \sin(\omega t) + 2aD\, A\, B^2 \sin(\omega t + \phi)], \tag{11b}$$

$$g_2 = a^2\, B\, (1 - 2\, a\, D\, B^2). \tag{11c}$$

In order to obey Eq. (10) each of the g_i must identically vanish. From the third condition $g_2 \equiv 0$ one readily obtains

$$B_{\pm} = \pm \frac{1}{\sqrt{2\, a\, D}}, \tag{12}$$

where only $B = B_+$ yields a physically relevant solution, since $p(x,t)$ is required to be normalized. Thus, one finds from $g_{0,1} \equiv 0$ with $B = B_+$ the necessary condition

$$A = \frac{S\, \sin(\omega t)}{B\omega\, \cos(\omega t + \phi) + S\, \sin(\omega t + \phi)}. \tag{13}$$

Since A is supposed to be constant we have

$$0 \overset{!}{=} \frac{d}{dt} A = \frac{S\omega[B\, \omega\, \cos(\phi) + \sin(\phi)]}{[B\omega\, \cos(\omega t + \phi) + S\, \sin(\omega t + \phi)]^2}, \tag{14}$$

which provides the required condition for the phase ϕ. Hence, we find

$$\phi = -\arctan(B\omega) = -\arctan\left(\frac{\omega}{\sqrt{2aD}}\right). \tag{15}$$

Inserting this result into Eq. (13) yields

$$A = \frac{S}{\sqrt{1 + B^2\omega^2}} = \frac{S}{\sqrt{1 + \omega^2/(2aD)}}. \tag{16}$$

By virtue of Eqs. (12), (15), and (16) we hereby have determined all parameters A, ϕ, and $B = B_+$ in the ansatz (9). It is now straightforward to calculate characteristic statistical quantities for this solution. For example, the mean value is obtained as

$$\overline{x}(t) = \frac{A}{a} \sin(\omega t + \phi), \tag{17}$$

and the variance becomes a constant,

$$\sigma^2(t) := \overline{x^2}(t) - \overline{x}(t)^2 = \frac{1}{aB} = \sqrt{\frac{2D}{a}}. \tag{18}$$

Performing the integration according to Eq. (2), the ensemble average of the fitness function $F(x,t)$ is obtained as

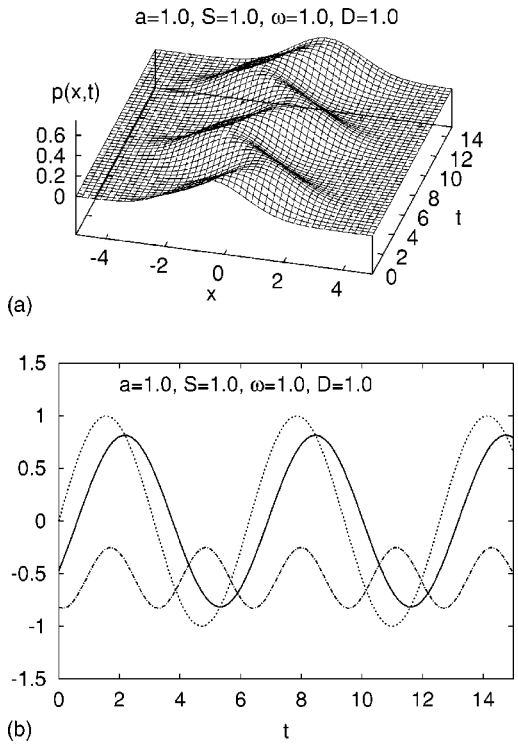

FIG. 1. (a) Plot of the analytic solution $p(x,t)$ for the periodically perturbed quadratic fitness function $F(x,t) = -0.5x^2 + x\, \sin(t)$. The parameters of the solution are $B = 0.71$, $\phi = -0.62$, and $A = 0.82$. (b) Mean value $\overline{x}(t)$ (solid line), driving signal $S\, \sin(\omega t)$ (dotted line), and ensemble fitness $\overline{F}(t)$ (dashed-dotted line) for same parameter values as in (a). One can readily observe that the phase shift ϕ, i.e., the mean value $\overline{x}(t)$ follows the perturbation signal with some retardation.

$$\overline{F}(t) = -\frac{1}{2B} + \frac{S^2}{4a(1 + B^2\omega^2)} + \frac{S^2}{4a(1 + B^2\omega^2)} \times (1 - 2\sqrt{1 + B^2\omega^2})\cos[2(\omega t + \phi)]. \tag{19}$$

Note that in contrast to the simple phase shift for $\overline{x}(t)$, the average $\overline{F}(t)$ oscillates with a frequency twice as large. Also note in this context that $\overline{F}(t)$ contains merely terms of order S^0 and S^2. In Fig. 1 we have plotted $p(x,t)$ together with a comparison between $\overline{x}(t)$, $\overline{F}(t)$, and the periodic perturbation.

We remark that the time-periodic asymptotic solution derived above is of the same Gaussian type as the solution of the Fokker-Planck system for the periodically driven harmonic oscillator. However, due to the different type of evolution equation, explicit differences consist for the phase shift ϕ, the response amplitude A, and the variance σ^2, as a comparison with the results of Refs. [24,32] shows.

B. Numerical methods

Unfortunately, for more complicated periodically driven fitness functions $F(x,t)$ it is generally impossible to find exact solutions by the procedure outlined in Sec. II A. Consequently, we present in Sec. IV A a perturbation theory approach which yields an approximative asymptotic solution of

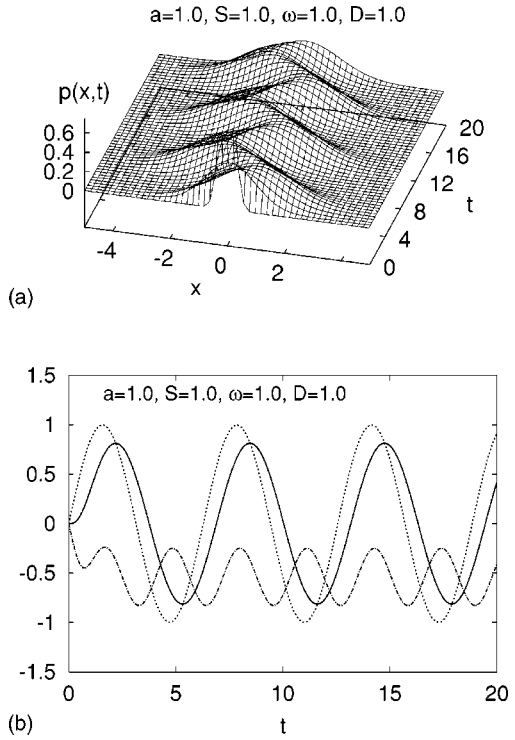

FIG. 2. (a) Plot of the numerical solution $p(x,t)$ of the PDE (1) for the periodically perturbed quadratic fitness function $F(x,t)=-0.5x^2+x\sin(t)$ and an initial distribution $p(x,0)=\delta(x)$. All parameters are the same as used in Fig. 1. (b) Driving signal $S\sin(\omega t)$ (dotted line), numerical calculated mean value $\overline{x}(t)$ (solid line), and ensemble fitness $\overline{F}(t)$ (dashed-dotted line) for the same parameter values as in (a). One can readily see how after a short relaxation time the system approaches the exact asymptotic solution plotted in Fig. 1. The details of the numerical algorithm can be found in the Appendix of Ref. [31].

the FEE (1). An alternative way to investigate more complicated cases consists in numerically integrating the PDE (1). In Secs. IV B and V we shall use the results of numerical simulations in order to test the predictions of the perturbation theory.

The exact details of the numerical algorithm used in all our simulations are explicitly described in the Appendix of Ref. [31]. Due to this fact, we confine ourselves here to a brief discussion of the most important aspects: The numerical integration scheme is based on a linear approximation of the partial derivatives, supplemented by a simple method that preserves non-negativity and normalization of the probability density. The algorithm was tested by comparing the numerical results (i) with (exact) analytical solutions of Eq. (1) that can be found for the special case of a nondriven ($S=0$) quadratic fitness function with Gaussian initial conditions (see Ref. [30] for an extensive discussion of these solutions); (ii) with the exact asymptotic solution derived in Sec. II A for the periodically driven ($S>0$) quadratic fitness function.

In all these tests the agreement between numerically and analytically calculated curves was very good; i.e., there was virtually no difference between the numerical and analytical results [e.g., compare Figs. 1(b) and 2(b)].

III. GENERAL SOLUTION OF THE FISHER-EIGEN EQUATION

Before perturbation theory is considered in Sec. IV, we shall discuss the generic solution of the FEE (1). It was already pointed out in the introduction that the Fisher-Eigen equation (1) is a nonlinear PDE. Interestingly enough, however, it can be transformed into a linear PDE, if one uses the ansatz [11,31]

$$p(x,t)=\varrho(x,t)\exp\left[-\int_0^t ds\overline{F}(s)\right], \tag{20}$$

satisfying at initial time $t=0$

$$p(x,0)=\varrho(x,0). \tag{21}$$

In contrast to $p(x,t)$, the non-negative function $\varrho(x,t)$ is *not* normalized. More precisely, one finds from Eq. (20) by means of an integration that

$$\tilde{Z}(t):=\int_G dx\varrho(x,t)=\exp\left[\int_0^t ds\overline{F}(s)\right], \tag{22}$$

and, thus, the general result

$$\overline{F}(t)=\frac{d}{dt}\ln\int_G dx\varrho(x,t)=\frac{d}{dt}\ln\tilde{Z}(t). \tag{23}$$

Inserting the ansatz (20) into the FEE (1) yields

$$\frac{\partial\varrho}{\partial t}=D\nabla^2\varrho+F(x,t)\varrho. \tag{24}$$

This equation deserves to be commented on: In the above approach, we started out from the FEE (1) and obtained Eq. (26) by applying the ansatz (20). Of course, one could instead also start from the rather general evolutionary equation (24), governing the dynamics of some *non-negative*, non-normalized density $\varrho(x,t)$. Then it is straightforward to show that the related *normalized* density $p(x,t)$, defined by

$$p(x,t)=\frac{\varrho(x,t)}{\int_G dx\varrho(x,t)}, \tag{25}$$

is governed by the Fisher-Eigen equation (1).

We now continue with the analysis of Eq. (24): In order to obtain a more familiar standard form we introduce two "potentials" by writing

$$U(x,t):=-F(x,t),\quad U_0(x):=-F_0(x). \tag{26}$$

These definitions allow us to recast Eq. (24) as

$$-\frac{\partial\varrho}{\partial t}=[-D\nabla^2+U(x,t)]\varrho. \tag{27}$$

The rhs of Eq. (27) has a Schrödinger-equation-like structure [33,34], though, compared with quantum mechanics a fundamental difference is given by the fact that the left-hand side is real valued. With regard to the subsequent discussion it is

convenient to introduce a time-dependent and time-periodic [23] operator

$$\hat{H}(t) := -D\nabla^2 + U(x,t) = -D\nabla^2 + U_0(x) - xS\sin\omega t, \tag{28}$$

obeying

$$\hat{H}(t) = \hat{H}(t+T) \tag{29}$$

with $T=2\pi/\omega$. Formally, the structure of the operator $\hat{H}(t)$ is very similar to that of a quantum-mechanical Hamilton operator (with parameters $\hbar=1$ and $2m=1/D$), which implies that a solution of Eq. (27) can be expressed in terms of eigenfunctions of $\hat{H}$. This will be discussed in the following two sections.

A. The case of no driving: $S=0$

Before we deal with the general case $S>0$, it might be useful to briefly consider the unperturbed problem $S=0$ first. Since an extensive discussion of this special case with regard to the Kramers transition problem can be found in Ref. [31], see also in Refs. [33,35], we shall merely present a summary of the main results.

Assuming a discrete, nondegenerate spectrum of eigenvalues, as it is the case for the examples considered below, the formal solution of the FEE (1) with $S=0$ is given by

$$p(x,t) = \exp\left[-\int_0^t ds\overline{F_0}(s)\right]\sum_{n=0}^{\infty} c_n\varphi_n(x)e^{-\lambda_n t}, \tag{30}$$

where φ_n is a $\mathcal{L}^2(G)$-normalized eigenfunction of the time-independent operator

$$\hat{H}_0 = -D\nabla^2 + U_0(x) \tag{31}$$

and λ_n is the corresponding eigenvalue, i.e.,

$$\delta_{mn} = \int_G dx\varphi_m^*(x)\varphi_n(x), \quad \hat{H}_0\,\varphi_n = \lambda_n\,\phi_n. \tag{32}$$

We have denoted by $\mathcal{L}^2(G)$ the space of square-integrable functions on G (where in our case $G=\mathbb{R}$). In view of Eq. (21) the coefficients

$$c_n = \int_G dx\varphi_n^*(x)p(x,0) \tag{33}$$

are determined by the initial condition. In order to identify the exponential prefactor in Eq. (30), one integrates Eq. (30) over x and makes use of the fact that $p(x,t)$ is normalized. This procedure yields

$$\exp\left[\int_0^t ds\overline{F_0}(s)\right] = \int_G dx\varrho(x,t) = \sum_{n=0}^{\infty} c_n l_n e^{-\lambda_n t}, \tag{34}$$

where we have defined the constants

$$l_n = \int_G dx\varphi_n(x). \tag{35}$$

Note that $l_n=0$ holds for $n=$odd, if the potential is symmetric, i.e. $U_0(x)=U_0(-x)$. From Eq. (34) it follows that

$$\overline{F_0}(t) = \frac{d}{dt}\ln\int_G dx\varrho(x,t) = -\frac{\sum_{n=0}^{\infty} c_n l_n\lambda_n e^{-\lambda_n t}}{\sum_{m=0}^{\infty} c_m\, l_m\, e^{-\lambda_m t}} \tag{36}$$

and

$$p(x,t) = \frac{\sum_{n=0}^{\infty} c_n\varphi_n(x)e^{-\lambda_n t}}{\sum_{m=0}^{\infty} c_m\, l_m\, e^{-\lambda_m t}}. \tag{37}$$

In conclusion, for the unperturbed case $S=0$ the solution of the FEE (1) can completely be given in terms of characteristic quantities of the eigenvalue problem (24).

Let us take a closer look at the stationary situation. Assuming a time-independent solution $p^s(x)$ of the FEE (1), we find from Eq. (36) that the stationary value $\overline{F_0^s}$ of $\overline{F_0}(t)$ is determined by the lowest eigenvalue

$$\overline{F_0^s} = -\lambda_0. \tag{38}$$

Moreover, due to Eq. (37), the stationary solution $p^s(x)$ is proportional to $\varphi_0(x)$, i.e.,

$$p^s(x) = \frac{\varphi_0(x)}{l_0}. \tag{39}$$

B. The case with nonzero driving: $S>0$

Generally, there exist many different methods to solve explicitly time-dependent problems of the type (27). To name only a few we mention here the Floquet formalism [36] and the Kramers-Henneberger oscillating frame representation [37,38], with the latter method widely applied in the theory of (rapidly) driven quantum problems [23].

In contrast, for our discussion we choose a more conventional, perturbative approach, which is based on the ansatz

$$\varrho(x,t) = \sum_{n=0}^{\infty}\varphi_n(x)c_n(t), \tag{40}$$

where the time-dependent coefficients are determined by

$$c_n(t) = \int_G dx\varphi_n^*(x)\varrho(x,t). \tag{41}$$

Because for all examples considered in this work the complete set of orthonormal eigenfunctions $\{\varphi_n\}$ of $\hat{H}_0$ are known to be real, we can drop from here on the asterisk in spatial scalar products such as Eq. (41). Inserting the ansatz (40) into the evolutionary equation (27) yields

$$\sum_{n=0}^{\infty}\left[\lambda_n - Sx\,\sin(\omega t) + \frac{d}{dt}\right]\varphi_n(x)c_n(t) = 0. \tag{42}$$

In order to obtain an ordinary differential equation (ODE) for each function $c_n(t)$ we multiply Eq. (42) by φ_k and integrate the resulting equation over x. This procedure yields

$$\dot{c}_k(t) + \lambda_k c_k(t) + S\,\sin(\omega t)\sum_{n=0}^{\infty} M_{kn}c_n(t) = 0, \tag{43}$$

where the matrix coefficients M_{kn} are given by

$$M_{kn} = -\int_G dx\varphi_k(x)x\varphi_n(x) = M_{nk}. \tag{44}$$

Due to the symmetry properties of the φ_n's in examples with symmetric fitness function, $F_0(x)=F_0(-x)$, we find that $M_{kn}=0$ holds whenever $n+k=$even.

It is now convenient to introduce in the following a matrix notation

$$\boldsymbol{c}(t) := [c_n(t)], \quad \boldsymbol{\varphi}(x) := [\varphi_n(x)],$$

$$\boldsymbol{M} := [M_{kn}], \quad \boldsymbol{\Lambda} := [\Lambda_{kn}] = [\lambda_k\delta_{kn}], \tag{45}$$

where $n,k=0,1,2,\ldots$. In this notation $\boldsymbol{c}(t)$ and $\boldsymbol{\varphi}(x)$ can be viewed as (infinite-dimensional) column vectors, whereas $\boldsymbol{M}$ and $\boldsymbol{\Lambda}$ represent matrices. These conventions allow us to rewrite the ansatz (40) in the form of a column vector scalar product

$$\langle\boldsymbol{\varphi}(x),\boldsymbol{c}(t)\rangle := \sum_{n=0}^{\infty}\varphi_n(x)c_n(t) = \varrho(x,t), \tag{46}$$

and, moreover, the ODE (43) as

$$\dot{\boldsymbol{c}}(t) = -[\boldsymbol{\Lambda} + S\,\sin(\omega t)\boldsymbol{M}]\boldsymbol{c}(t), \tag{47}$$

where, for example,

$$\boldsymbol{M}\boldsymbol{c}(t) := \left[\sum_{i=0}^{\infty} M_{ni}c_i(t)\right] \tag{48}$$

yields again a column vector. The well-known formal solution of Eq. (49) is given by

$$\boldsymbol{c}(t) = \hat{\mathfrak{J}}\exp\left\{-\int_0^t ds[\boldsymbol{\Lambda} + S\,\sin(\omega s)\boldsymbol{M}]\right\}\boldsymbol{c}(0), \tag{49}$$

where $\hat{\mathfrak{J}}$ denotes the time-ordering operator. Introducing the abbreviation

$$\boldsymbol{A}(t) = -[\boldsymbol{\Lambda} + S\,\sin(\omega t)\boldsymbol{M}], \tag{50}$$

Eq. (49) is, by definition, equivalent to

$$\boldsymbol{c}(t) = \left[\mathbf{1} + \sum_{i=1}^{\infty}\int_0^t dt_1\int_0^{t_1}\cdots\int_0^{t_{i-1}} dt_i \times\boldsymbol{A}(t_1)\boldsymbol{A}(t_2)\cdots\boldsymbol{A}(t_i)\right]\boldsymbol{c}(0), \tag{51}$$

where $\mathbf{1}$ denotes the unity matrix. The diagonal matrix $\boldsymbol{\Lambda}$ does not commute with $\boldsymbol{M}$ and, therefore, also the matrices $\boldsymbol{A}(t_i)$ do generally not commute. More precisely, the matrix elements of the commutator

$$[\boldsymbol{M},\boldsymbol{\Lambda}] := \boldsymbol{M}\boldsymbol{\Lambda} - \boldsymbol{\Lambda}\boldsymbol{M} \tag{52}$$

can be evaluated to read

$$[\boldsymbol{M},\Lambda]_{ij} = \sum_{n=0}^{\infty}(M_{in}\lambda_n\delta_{nj} - \lambda_i\delta_{in}M_{nj}) = (\lambda_j - \lambda_i)M_{ij}. \tag{53}$$

However, it is straightforward to determine $\boldsymbol{c}(0)=[c_n(0)]$ in Eq. (51) from the initial conditions, since at time $t=0$ we have by virtue of Eq. (21)

$$\varrho(x,0) = \sum_{n=0}^{\infty}\varphi_n(x)c_n(0) = p(x,0). \tag{54}$$

In view of the orthogonality of the set $\{\varphi_n\}$ we find

$$c_n(0) = \int_G dx\varphi_n(x)p(x,0). \tag{55}$$

In particular, the choice of special initial conditions can simplify further calculations, e.g., for $p(x,0)\sim\varphi_0(x)$ we have $c_{n\neq 0}(0)=0$.

In terms of the scalar product (46), we can summarize the formal solutions for $p(x,t)$ and $\overline{F}(t)$ by

$$p(x,t) = \frac{\langle\boldsymbol{\varphi}(x),\boldsymbol{c}(t)\rangle}{\tilde{Z}(t)}, \quad \tilde{Z}(t) = \langle\boldsymbol{l},\boldsymbol{c}(t)\rangle \tag{56}$$

and

$$\overline{F}(t) = \frac{d}{dt}\ln\tilde{Z}(t), \tag{57}$$

where we used, for convenience, $\boldsymbol{l}=[l_n]$ with l_n defined by Eq. (35). By means of Eq. (47) one can also rewrite Eq. (57) as

$$\overline{F}(t) = \frac{\langle\boldsymbol{l},\boldsymbol{A}(t)\boldsymbol{c}(t)\rangle}{\langle\boldsymbol{l},\boldsymbol{c}(t)\rangle}. \tag{58}$$

We are thus able to formally write down the exact solutions for $p(x,t)$ and $\overline{F}(t)$. Even though the above outlined formal theory in addition possesses merit for numerical studies, these results are of limited use in practice in order to describe specific quantitative results. A natural obstacle is, for example, that one usually does not have knowledge of the exact eigenfunctions φ_n of the unperturbed problem and, as well, of related quantities such as the matrix elements M_{kn} and the

set of eigenvalues λ_k. In the following we shall therefore pursue an approximation scheme which will enable us to estimate the relevant asymptotic behavior of the system dynamics to leading order in the driving strength (linear response approximation).

IV. PERTURBATION THEORY

The first aim of this part is to derive a perturbation expansion that yields approximate solutions for the asymptotic density $p^a(x,t)$ and the asymptotic mean value $\overline{x^a}(t)$. This will be done in Sec. IV A. Subsequently, in Sec. IV B, these results are applied to the single-peaked quadratic and the single-peaked quartic fitness function, respectively.

During the following discussion, we restrict ourselves to situations for which the time-independent part $F_0(x)$ of the fitness function $F(x,t)$ satisfies the symmetry property $F_0(-x)=F_0(x)$. Moreover, we demand as before that the spectrum of the related operator $\hat{H}_0$ is discrete and nondegenerate.

A. Small *S* expansion

We attempt to expand the problem with respect to powers of the signal strength S. To this end we assume that we can write the solution of the perturbed problem in the form

$$\varrho(x,t)=\sum_{i=0}^{\infty} S^i \varrho_i(x,t). \tag{59}$$

Inserting this ansatz into Eq. (27) yields

$$-\sum_{i=1}^{\infty} S^i \frac{\partial}{\partial t}\varrho_i=\sum_{i=0}^{\infty} S^i[-D\nabla^2+U_0(x)-xS\,\sin(\omega t)]\varrho_i. \tag{60}$$

Considering the contributions of order S^i separately, we obtain the following hierarchy of equations:

$$\frac{\partial}{\partial t}\varrho_0=[D\nabla^2-U_0(x)]\varrho_0, \tag{61}$$

$$\frac{\partial}{\partial t}\varrho_i=[D\nabla^2-U_0(x)]\varrho_i+x\,\sin(\omega t)\varrho_{i-1} \tag{62}$$

for $i=1,2,\ldots$. Apparently, $\varrho_0(x,t)$ is simply the solution of the unperturbed problem and, therefore, asymptotically (superscript a)

$$\varrho_0^a(x,t)=\exp(-\lambda_0 t)\varphi_0(x), \tag{63}$$

and, thus,

$$p^a(x,t)=\frac{\varphi_0(x)}{l_0}+\mathcal{O}(S)=p^s(x)+\mathcal{O}(S). \tag{64}$$

Next, we consider the dynamics of $\varrho_1^a(x,t)$. A plausible ansatz reads

$$\varrho_1^a(x,t)=\sum_{i=0}^{\infty} a_{1i}(t)e^{-\lambda_0 t}\varphi_i(x). \tag{65}$$

In view of the orthonormality of the φ_i we find the following ODE for the time-dependent coefficients

$$\dot{a}_{1i}(t)=-\gamma_i a_{1i}(t)-\sin(\omega t)M_{i0}, \tag{66}$$

where

$$\gamma_i:=\lambda_i-\lambda_0. \tag{67}$$

In particular, we observe that $\dot{a}_{10}(t)\equiv 0$ holds for a symmetric fitness function. The asymptotic solution of Eq. (66) for $i=1,2,\ldots$ can be written as

$$a_{1i}(t)=M_{i0}\left[\frac{\omega}{\gamma_i^2+\omega^2}\cos(\omega t)-\frac{\gamma_i}{\gamma_i^2+\omega^2}\sin(\omega t)\right]. \tag{68}$$

Consequently, due to $M_{(2j)0}=0$ for symmetric problems, only terms with odd numbered i's contribute in Eq. (65), yielding

$$p^a(x,t)=\frac{1}{l_0}\left\{\varphi_0(x)+S\sum_{i=1}^{\infty} M_{i0}\left[\frac{\omega}{\gamma_i^2+\omega^2}\cos(\omega t)-\frac{\gamma_i}{\gamma_i^2+\omega^2}\sin(\omega t)\right]\varphi_i(x)\right\}+\mathcal{O}(S^2). \tag{69}$$

Thus, we find for the linear response [1,33,39,40] of the related asymptotic mean value the result

$$\overline{x^a}(t)=S\sum_{i=1}^{\infty}\frac{\mu_i M_{i0}}{l_0}\left[\frac{\omega}{\gamma_i^2+\omega^2}\cos(\omega t)-\frac{\gamma_i}{\gamma_i^2+\omega^2}\sin(\omega t)\right]+\mathcal{O}(S^2), \tag{70}$$

where

$$\mu_i:=\int_G dx x\varphi_i(x). \tag{71}$$

Put differently, given the eigenvalue differences $\gamma_i=\lambda_i-\lambda_0$ and the eigenfunctions $\varphi_i(x)$ of the unperturbed problem, we can describe the linear response of the asymptotic system dynamics. Moreover, if the eigenvalue differences γ_i are strongly increasing for $i=1,2,\ldots$, then it should even be sufficient to merely consider the λ_1 contribution in Eq. (70), i.e.,

$$\overline{x_1^a}(t)\approx S\frac{\mu_1 M_{10}}{l_0}\left[\frac{\omega}{\gamma_1^2+\omega^2}\cos(\omega t)-\frac{\gamma_1}{\gamma_1^2+\omega^2}\sin(\omega t)\right]=:\overline{x_1^a}(t). \tag{72}$$

This can still be simplified to

$$\overline{x_1^a}(t)=-\frac{\mu_1}{l_0}\frac{SM_{10}}{\sqrt{\gamma_1^2+\omega^2}}\sin(\omega t-\phi), \tag{73}$$

where the phase shift is given by

$$\phi = \arctan\left(\frac{\omega}{\gamma_1}\right). \tag{74}$$

The related amplitude function

$$\chi_{10} := \frac{1}{S}\max_t \overline{x_1^a}(t) = -\frac{\mu_1}{l_0}\frac{M_{10}}{\sqrt{\gamma_1^2+\omega^2}} \tag{75}$$

will be referred to as *partial response amplitude* in the following. This very quantity will be invoked below to characterize the spectral amplification for stochastic resonance [1,41]. In particular, we shall compare analytical estimates for χ_{10} with numerical results for the *total response amplitude*

$$\chi_{tot} := \frac{1}{S}\max_t \overline{x^a}(t), \tag{76}$$

defined as the ratio between the amplitude of $\overline{x^a}(t)$ and the driving amplitude S. In contrast to χ_{10}, for quartic fitness functions the total amplitude χ_{tot} can only be determined by means of computer simulations, since the exact solution $\overline{x^a}(t)$ remains unknown.

B. Application to single-peaked fitness functions

We shall now apply the results of the preceding section to two simple examples, representing single-peaked fitness functions. From these applications it will become clear that the partial response amplitude χ_{10} from Eq. (75) can be used to predict the appearance of stochastic resonance in the FEM.

Before we start discussing the first example, the following remark is in order: Since we intend to calculate χ_{10}, we must know the quantities μ_1, l_0, M_{10}, and γ_1, which follow from the first two eigenfunctions and eigenvalues of the unperturbed operator $\hat{H}_0$. Unfortunately, for arbitrary fitness functions the eigenvalue problem for $\hat{H}_0$ cannot be solved exactly and one has to use, for example, standard variational methods [42,43]. For fitness functions $F_0(x)$ possessing a single maximum or for corresponding potentials $U_0(x)=-F_0(x)$ exhibiting a single minimum, respectively, it is appropriate to use the orthogonal, normalized test functions

$$\varphi_0(x) = \left(\frac{2\alpha}{\pi}\right)^{1/4}\exp(-\alpha x^2),$$

$$\varphi_1(x) = 2\left(\frac{2\alpha^3}{\pi}\right)^{1/4} x\,\exp(-\alpha x^2) \tag{77}$$

as approximations of the first two eigenfunctions, where α is the variational parameter. These test functions yield

$$l_0 = \left(\frac{2\pi}{\alpha}\right)^{1/4}, \quad \mu_1 = \left(\frac{2\pi}{\alpha^3}\right)^{1/4}, \quad M_{10} = -\frac{1}{2\sqrt{\alpha}}, \quad \gamma_1 = 4D\alpha. \tag{78}$$

These results are valid whenever test functions of the form (77) are applied. In particular this implies that in the case of a quadratic fitness function or potential these become exact.

1. Quadratic fitness function

Let us first consider the quadratic fitness function $F_0(x) = -ax^2/2$ as discussed in Sec. II. In this case, we can make use of the well-known results for the eigenvalues and dipole moments of the quantum harmonic oscillator [37], yielding

$$\lambda_n = \sqrt{2aD}\left(n+\frac{1}{2}\right) \tag{79}$$

and

$$M_{kn} = -\left(\frac{D}{2a}\right)^{1/4}(\delta_{k(n-1)}\sqrt{n} + \delta_{k(n+1)}\sqrt{n+1}). \tag{80}$$

Thus, we have

$$\alpha = \sqrt{\frac{a}{8D}}, \quad \gamma_n = n\sqrt{2aD}, \quad \frac{\mu_1}{l_0} = \left(\frac{8D}{a}\right)^{1/4},$$

$$M_{10} = -\left(\frac{D}{2a}\right)^{1/4}. \tag{81}$$

Since according to Eq. (82) also $M_{i0}=0$ for $i>1$ holds, the linear response result (70) for the harmonic potential coincides with the exact result (17) given in Sec. II. In particular, for the quadratic fitness function the partial response amplitude χ_{10} precisely equals the total response amplitude χ_{tot}. We also remark that for a quadratic fitness function there exists no optimal diffusion strength D; put differently, the related partial response amplitude $\chi_{10}=\chi_{tot}$ exhibits a monotonically increasing behavior towards saturation, see Fig. 3(a). Consequently, stochastic resonance cannot occur for this particular example.

2. Quartic fitness function

We now consider the fitness function

$$F_0(x) = -g\frac{x^4}{4}, \quad g>0. \tag{82}$$

For Eq. (82) the optimization parameter α is explicitly determined as

$$\alpha = \frac{1}{2}\left(\frac{3g}{4D}\right)^{1/3}, \tag{83}$$

yielding for the linear response amplitude the result

$$\chi_{10} = \left(\frac{4D}{3g}\right)^{1/3}\frac{1}{\sqrt{(6D^2g)^{2/3}+\omega^2}}. \tag{84}$$

Thus, in contrast to the case with a quadratic fitness function, there exists now an optimal value

$$D_c = \sqrt{\frac{\omega^3}{6g}}, \tag{85}$$

for which the partial amplitude χ_{10} assumes a maximum. This can be interpreted as the appearance of *stochastic resonance* in the Fisher-Eigen model. In Fig. 3 we depict the spectral amplification measure [41,44] χ_{10} for different val-

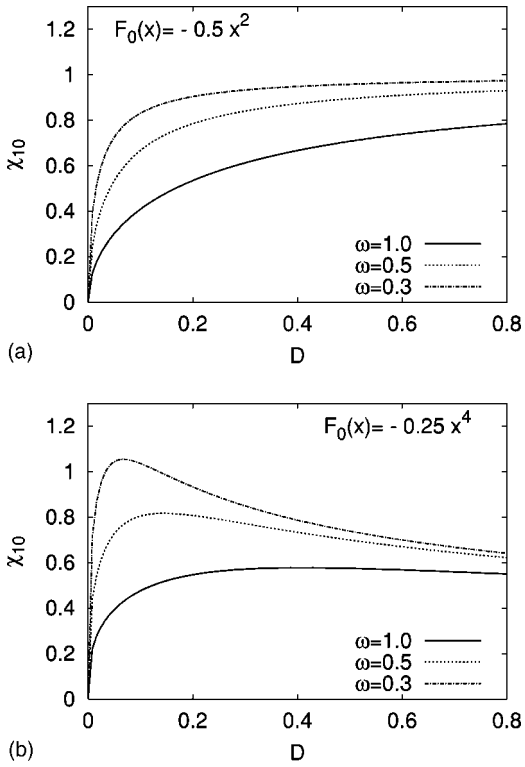

FIG. 3. Partial response amplitudes χ_{10} for (a) the single-peaked quadratic fitness function $F_0(x)=-0.5x^2$, and for (b) the single-peaked quartic fitness function $F_0(x)=-0.25x^4$ at different driving frequencies ω. For the quartic weighting factor $g=1$, see Eq. (82), the maxima of χ_{10} in (b) are located at the values $D_c=\sqrt{\omega^3/6}$. Thus, linear perturbation theory predicts that stochastic resonance is absent in the case of the harmonic fitness function, but likely to occur for the quartic fitness function.

ues of ω. However, in order to (numerically) prove whether the FEM indeed does exhibit the stochastic resonance behavior with quartic fitness function we performed numerical calculations. This is so, because infinitely many contributions stemming from higher-order eigenfunctions of the, in this case, nonvanishing matrix elements $M_{30}, M_{50}, \ldots$ towards the full amplitude χ_{tot} have been neglected.

Nevertheless, this preliminary result does indicate that the nonlinearity of the fitness function plays a decisive role for the possible occurrence of the stochastic resonance phenomenon: The results of the numerical simulations, shown in Fig. 4, indeed confirm that stochastic resonance does occur. One should, however, also note that the numerically found values χ_{tot} are quantitatively not well fitted by the linear response result χ_{10}. According to our opinion this deviation is due to the following two reasons: On the one hand, as already pointed out above, the total amplitude χ_{tot} also contains contributions of higher matrix elements $M_{30}, M_{50}, \ldots$ that are neglected in χ_{10}. On the other hand, the quality of the approximation χ_{10} is also limited by the quality of the applied test functions. In other words, better estimates of the true eigenfunctions are likely to result in a better agreement between χ_{tot} and χ_{10}.

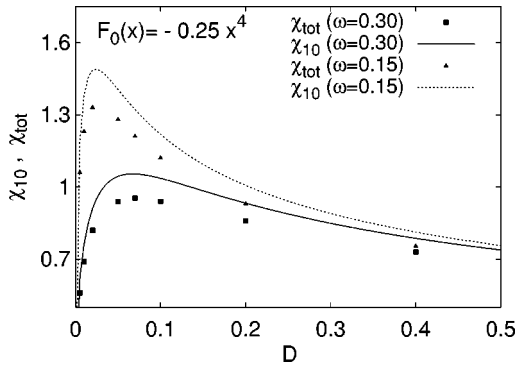

FIG. 4. Comparison between numerically calculated values of the total amplitude χ_{tot} (filled squares and triangles) and analytical curves χ_{10} (solid and dotted lines) for the quartic fitness function $F(x,t)=-0.25gx^4+Sx\sin(\omega t)$ with parameters $g=1$ and $S=0.1$. From inspection, the numerical results do confirm the stochastic resonance effect predicted by the partial amplitude χ_{10}, which is a result of first-order perturbation theory in S.

V. DOUBLE-PEAKED FITNESS FUNCTION

A. Introductory remarks

In the remainder of this work we now concentrate on the archetypal driven model of a bistable fitness function, i. e.,

$$F(x,t)=\frac{a}{2}x^2-\frac{b}{4}x^4+xS\sin\omega t, \quad a,b,S>0, x\in\mathbb{R}. \tag{86}$$

(As before we shall assume that all quantities are given in scaled, dimensionless form.) In the context of stochastic resonance (SR) and stochastic synchronization, this problem has been extensively studied for Fokker-Planck and quantum processes during the past two decades [1–3,21,23,45]. The phenomenon of SR originated from its possible role in the explanation for the periodically recurrent climatic changes [1,46,47]. Here we deal with the question whether a similar, noise-induced phenomenon may occur in biological systems described by the Fisher-Eigen evolution equation in Eq. (1).

With regard to biological evolution, the bistable model fitness function (86) describes the following situation.

First, let us consider the nondriven case, i.e., $S=0$. Then the fitness function (86) assumes the time-independent shape

$$F_0(x)=\frac{a}{2}x^2-\frac{b}{4}x^4. \tag{87}$$

Thus, for some biological species described by F_0 there exist two states of maximal fitness at $x=\pm x_m$, corresponding to two different phenotypes, where

$$x_m=\sqrt{\frac{a}{b}}. \tag{88}$$

In the equilibrium situation most members of the species will possess a phenotype close to either $+x_m$ or $-x_m$. Deviations from the optimal phenotypes $\pm x_m$ are due to mutations. Furthermore, since F_0 is symmetric, the corresponding time-

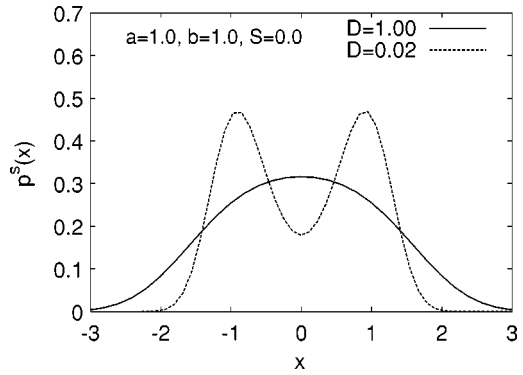

FIG. 5. Numerically calculated stationary solution $p^s(x)$ of Eq. (89) for the unperturbed system with $S=0$. Depending on the mutation parameter D the stationary distribution can either possess one central peak or two symmetric peaks.

independent equilibrium distribution $p^s(x)$, which is defined as the solution of

$$0 = [F_0(x) - \overline{F_0^s}]p(x) + D\nabla^2 p(x), \tag{89}$$

is also symmetric, $p^s(x)=p^s(-x)$. As illustrated in Fig. 5, the explicit shape of the stationary distribution $p^s(x)$ essentially depends on the size of the mutation (diffusion) parameter D.

Considering the influence of external driving, $S>0$, the explicitly time-dependent part in Eq. (86) can be interpreted as some weak external perturbation, which periodically improves or decreases the fitness values of certain phenotypes. Typical candidates for such effects could be periodic climate changes in biological systems, or also market cycles in economic systems, to name but a few. Regarding such phenomena, one should expect that the driving period

$$T = \frac{2\pi}{\omega}, \tag{90}$$

characterizing the time scale of the external perturbation, is very large compared with the lifetime of members of the species. Hence, in such cases both S and ω will be very "small" parameters, intuitively justifying the use of the perturbation theory outlined above.

In the following section we shall discuss results that have been obtained by applying this perturbation theory to the Fisher-Eigen equation (1) for the double-peaked fitness function (86). Beforehand, it is useful to introduce the scaled quantities

$$\tilde{x} = \frac{x}{x_m}, \quad \tilde{t} = tax_m^2, \quad \tilde{D} = \frac{D}{ax_m^4},$$

$$\tilde{S} = \frac{S}{ax_m}, \quad \tilde{\omega} = \frac{\omega}{ax_m^2}, \quad \tilde{p}(\tilde{x},\tilde{t}) = x_m\, p(x,t). \tag{91}$$

This is equivalent to setting $a=b=1$. For the sake of convenience we drop all tildes to obtain the following rescaled version of the Fisher-Eigen equation (1):

$$\frac{\partial p}{\partial t} = [F - \overline{F}(t)]p + D\nabla^2 p, \tag{92}$$

where the rescaled fitness function takes the form

$$F(x,t) = \frac{x^2}{2} - \frac{x^4}{4} + x\, S\, \sin(\omega t). \tag{93}$$

B. Results of perturbation theory

In the following we shall determine estimates for the partial response amplitude χ_{10} in the two limiting cases of strong and weak diffusion D. According to Sec. IV, for this purpose we need to evaluate the quantities M_{10}, l_0, μ_1, and γ_1 for the operator

$$\hat{H}_0 = -D\nabla^2 + \frac{x^4}{4} - \frac{x^2}{2}. \tag{94}$$

1. Strong diffusion limit

In the strong diffusion limit $D\to\infty$, the influence of the central well of the fitness function on the dynamics of the system becomes negligible. This fact is also illustrated by Fig. 5, where it can be deduced that for large values of D, the stationary distribution of the unperturbed problem exhibits only a single maximum at $x=0$. The explanation for this result is that due to the strong diffusion or dominating mutations, respectively, large parts of the population occupy phenotype regions with low fitness values. Therefore, if we neglect the central well of the fitness functions, which is caused by the quadratic term in $F_0(x)$, we are in the position to apply the stochastic resonance results for the quartic fitness function derived in Sec. IV B 2, cf. Fig. 4. In particular, Eq. (85) implies that stochastic resonance effects may only be observable if the driving frequency ω is *sufficiently large*.

In terms of the eigenvalue spectrum of the related operator $\hat{H}_0$ with potential $U_0(x)=-F_0(x)$, the condition of "strong diffusion" can be conceived as follows:

$$\lambda_0 \gg U_0(0) = 0, \tag{95}$$

where $x_0=0$ is the position of the local maximum of $U_0(x)$. On the other hand, if there exist sufficiently many eigenvalues $\lambda_0<\lambda_1<\cdots<\lambda_n$, such that

$$\lambda_n < 0, \tag{96}$$

then we shall speak of the "weak diffusion limit." This convention is in agreement with the notion of "deep" and "shallow" potentials in quantum mechanics.

2. Weak diffusion limit

For the opposite limit of weak diffusion $D\to 0$, corresponding to deep potentials (that is, potentials with a high barrier), there exist several methods to obtain the quantities M_{10}, l_0, μ_1, and γ_1. As before in Sec. IV B 2, we put the variational method to work, using the orthogonal functions

$$\varphi_0(x) = \frac{\mathcal{N}_0}{\sqrt{2}}\{\exp[-\alpha(x-1)^2] + \exp[-\alpha(x+1)^2]\}, \tag{97a}$$

$$\varphi_1(x) = \frac{\mathcal{N}_1}{\sqrt{2}}\{\exp[-\alpha(x-1)^2] - \exp[-\alpha(x+1)^2]\} \tag{97b}$$

as approximations of the first two eigenfunctions, where α is the variational parameter and

$$\mathcal{N}_0 = \left[\sqrt{\frac{\pi}{2\alpha}}(1+e^{-2\alpha})\right]^{-1/2}, \quad \mathcal{N}_1 = \left[\sqrt{\frac{\pi}{2\alpha}}(1-e^{-2\alpha})\right]^{-1/2} \tag{98}$$

are normalization constants. These test functions yield

$$l_0 = \left(\frac{8\pi}{\alpha}\right)^{1/4}\frac{1}{\sqrt{1+e^{-2\alpha}}}, \quad \mu_1 = \left(\frac{8\pi}{\alpha}\right)^{1/4}\frac{1}{\sqrt{1-e^{-2\alpha}}},$$

$$M_{10} = -\frac{1}{\sqrt{1-e^{-4\alpha}}} \tag{99}$$

and the eigenvalue difference emerges as

$$\gamma_1 = \frac{3-2\alpha+32\alpha^3 D}{8\alpha\,\sinh(2\alpha)}. \tag{100}$$

Hence, the partial response amplitude χ_{10} can be written as

$$\chi_{10} = \frac{1+\coth(\alpha)}{2\sqrt{\gamma_1^2+\omega^2}}. \tag{101}$$

Unfortunately, for the operator (94) the optimization parameter α cannot be calculated analytically, because the Ritz variational condition leads to a transcendental equation for α. Using a harmonic approximation near the minima of $U_0(x)$ yields

$$\alpha = \sqrt{\frac{|U_0''(x_m)|}{8D}} = \sqrt{\frac{1}{4D}}, \tag{102}$$

and, therefore,

$$\gamma_1 = \frac{3(\sqrt{D}+1)}{4\,\sinh(1/\sqrt{D})}. \tag{103}$$

In Fig. 6 we depict the comparison between the partial amplitude χ_{10}, based on this estimate of γ_1, and the numerically calculated full amplitude χ_{tot}. As seen from Fig. 6(a), the partial amplitude result does predict the existence of a stochastic resonance regime, provided that the driving frequency ω is *sufficiently large*. The corresponding numerical results for the total response amplitude χ_{tot} confirm this theoretical prediction. This becomes clear from Fig. 6(b), where the lines with $\omega \leqslant 0.5$ exhibit a monotonically decreasing behavior. In contrast, the curves with $\omega=0.7$ and $\omega=1.0$ show a weak local maximum; i.e., stochastic resonance characteristics are emerging for this set of parameters. In particular, these observations provide evidence that, in principle, also in the weak diffusion limit the simple (two-eigenfunction) linear response approximation can be used to predict whether stochastic resonance for the bistable quartic fitness function in fact occurs. The significant quantitative deviation of the analytical estimates χ_{10} in Fig. 6(a) from the exact (numerically determined) values χ_{tot} in Fig. 6(b) is due to the same reasons as discussed at the end of Sec. IV B 2. In particular, the breakdown of the perturbation theory for $D \to 0$ comes as no surprise, for it was recently shown [39,40] that applicability of the linear response method is restricted to the parameter region $D/S \gg 1$.

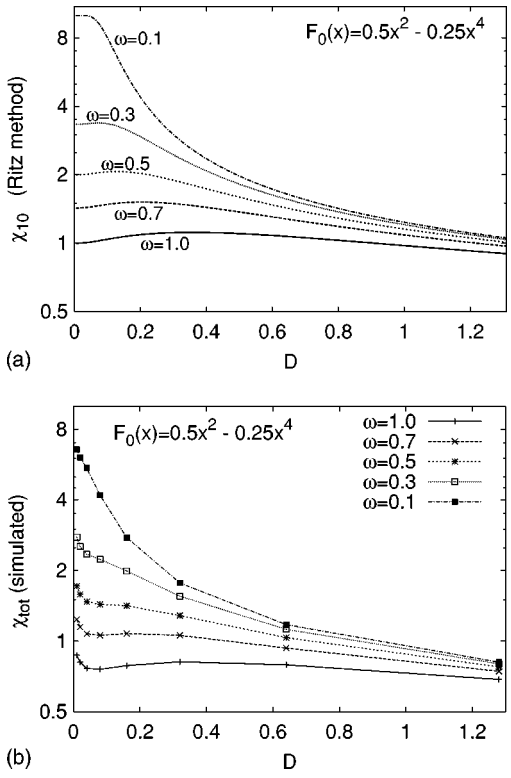

FIG. 6. Stochastic resonance in the weak diffusion limit for the double-peaked fitness function $F(x,t)=0.5x^2-0.25x^4+x\,S\,\sin(\omega t)$. Diagrams (a) shows the analytical linear response estimates for the partial amplitude χ_{10}, obtained by applying the Ritz method. Diagram (b) depicts the corresponding numerically calculated total amplitude χ_{tot} for driving parameters $S=0.1$. According to diagram (a), the analytical estimates for χ_{10} indicate the possibility of stochastic resonance provided the driving frequency is *sufficiently large*, $\omega > 0.1$. As shown in (b), the numerical results confirm the existence of a weak stochastic resonance effect in the case of external high frequency driving, i.e., for $\omega \geqslant 0.7$.

VI. CONCLUSIONS

In this work, the phenomenon of stochastic resonance in the FEM has been identified. In the FEM the evolutionary dynamics of an ensemble is governed by a global coupling. Therefore, the dynamical equation of this model has the form of a nonlinear partial differential equation for the population density and is composed of a homogeneous part and a diffu-

sive part. The dynamics of the nonlinear Fisher-Eigen equation can equivalently be mapped onto a linear equation. Thus, the occurrence in this type of nonlinear master equation is distinctly different from stochastic resonance in globally coupled Fokker-Planck mean-field-type situations [16] and also distinct from the phenomenon of spatiotemporal stochastic resonance in coupled nonlinear, dynamical, and excitable systems [48–52]. It could be shown both analytically and numerically that in the presence of periodic driving the FEM can feature stochastic resonance effects.

In particular, we have calculated the exact asymptotic solution for the case of a simple quadratic fitness function with sinusoidal driving. A main finding is that for this quadratic fitness function stochastic resonance effects do *not* occur. In contrast, for the more complicated case of a single-peaked, quartic fitness function (Sec. IV B 2) stochastic resonance is observable. Moreover, this phenomenon can be quantitatively understood within the framework of linear response theory. For example, one is able to calculate a satisfactory analytic estimate for the critical diffusion strength D_c, at which the resonance occurs.

According to the results of Sec. V, linear response theory can also be used in order to predict stochastic resonance effects in the case of a double-peaked, quartic fitness function. Here, a weak stochastic resonance effect is observable only if the frequency of the external signal is sufficiently large. This result follows from the linear perturbation theory with respect to the driving amplitude S, and has been corroborated by numerical simulations of the Fisher-Eigen equation. We therefore conclude that, although the quantitative agreement is essentially limited by the quality of required eigenvalue approximations, linear response methods in principle provide a useful tool to predict the appearance of stochastic resonance in the FEM.

ACKNOWLEDGMENTS

This work was supported by the DFG via the collaborative research project SFB 555 (L.S.-G.), by the Studienstiftung des deutschen Volkes (J.D.), by the Friedrich-Naumann-Stiftung (S.H.), and by the collaborative research project of the DFG, SFB 486, Project No. A.10 (P.H.).

[1] L. Gammaitoni, P. Hänggi, P. Jung, and F. Marchesoni, Rev. Mod. Phys. **70**, 223 (1998).
[2] V. S. Anishenko, A. B. Neiman, F. Moss, and L. Schimansky-Geier, Usp. Fiz. Nauk **169**, 7 (1999) [Phys. Usp. **42**, 7 (1999)].
[3] P. Hänggi, ChemPhysChem **3**, 285 (2002).
[4] I. E. Dikshtein, D. V. Kusnetsov, and L. Schimansky-Geier, Phys. Rev. E **65**, 061101 (2002).
[5] R. D. Astumian and P. Hänggi, Phys. Today **55**(11), 33 (2002).
[6] P. Reimann and P. Hänggi, Appl. Phys. A: Mater. Sci. Process. **75**, 169 (2002).
[7] F. Jülicher, A. Ajdari, and J. Prost, Rev. Mod. Phys. **69**, 1269 (1997).
[8] P. Reimann, Phys. Rep. **361**, 57 (2002).
[9] R. A. Fisher, *The Genetical Theory of Natural Selection* (Oxford University Press, Oxford, 1930).
[10] M. Eigen, Naturwissenschaften **58**, 465 (1971).
[11] R. Feistel and W. Ebeling, *Evolution of Complex Systems* (Kluwer Academic, Dordrecht, 1989).
[12] W. Ebeling and A. Engel, Syst. Anal. Model. Simul. **3**, 377 (1986).
[13] R. Feistel and W. Ebeling, BioSystems **15**, 291 (1982).
[14] S. Shinomoto and Y. Kuramoto, Prog. Theor. Phys. **75**, 1105 (1986).
[15] M. Shiino, Phys. Rev. A **36**, 2393 (1987).
[16] P. Jung, U. Behn, E. Pantazelou, and F. Moss, Phys. Rev. A **46**, R1709 (1992).
[17] S. H. Park and S. Kim, Phys. Rev. E **53**, 3425 (1996).
[18] P. Reimann, R. Kawai, C. V. den Broeck, and P. Hänggi, Europhys. Lett. **45**, 545 (1999).
[19] J. H. Li and P. Hänggi, Phys. Rev. E **64**, 011106 (2001).
[20] M. Kostur, J. Luczka, and L. Schimansky-Geier, Phys. Rev. E **65**, 051115 (2002).
[21] J. A. Freund, L. Schimansky-Geier, and P. Hänggi, Chaos **13**, 225 (2003).
[22] J. A. Freund, A. B. Neiman, and L. Schimansky-Geier, Europhys. Lett. **50**, 8 (2000).
[23] M. Grifoni and P. Hänggi, Phys. Rep. **304**, 229 (1998).
[24] P. Hänggi, P. Jung, C. Zerbe, and F. Moss, J. Stat. Phys. **70**, 25 (1993).
[25] T. Asselmeyer, W. Ebeling, and H. Rosé, Phys. Rev. E **56**, 1171 (1997).
[26] *Dynamik, Evolution, Strukturen-Nichtlineare Dynamik und Statistik komplexer Strukturen*, edited by J. A. Freund, Wissenschaftliche Schriftenreihe Physik Vol. 50 (Verlag Dr. Köster, Berlin, 1996).
[27] F. Schweitzer, W. Ebeling, H. Rosé, and O. Weiss, Evol. Comput. **5**, 419 (1998).
[28] T. Boseniuk, W. Ebeling, and A. Engel, Phys. Lett. A **125**, 307 (1987).
[29] T. Asselmeyer and W. Ebeling, BioSystems **41**, 167 (1996).
[30] J. Dunkel, L. Schimansky-Geier, and W. Ebeling, Evol. Comput. **12**, 1 (2004).
[31] J. Dunkel, W. Ebeling, L. Schimansky-Geier, and P. Hänggi, Phys. Rev. E **67**, 061118 (2003).
[32] P. Jung and P. Hänggi, Phys. Rev. A **41**, 2977 (1990).
[33] P. Hänggi and H. Thomas, Phys. Rep. **88**, 207 (1982).
[34] L. F. Favella, Ann. Inst. Henri Poincare, Anal. Non Lineaire **7**, 77 (1967).
[35] P. Hänggi, P. Talkner, and M. Borkovec, Rev. Mod. Phys. **62**, 251 (1990).
[36] G. Floquet, Ann. Sci. Ec. Normale Super. **12**, 47 (1883).
[37] H. A. Kramers, *Quantum Mechanics* (North-Holland, Amsterdam, 1956).
[38] W. C. Henneberger, Phys. Rev. Lett. **21**, 838 (1968).
[39] J. Casado-Pascual, J. Gomez-Ordonez, M. Morillo, and P. Hänggi, Europhys. Lett. **58**, 242 (2002).
[40] J. Casado-Pascual, C. Denk, J. Gomez-Ordonez, M. Morillo,

and P. Hänggi, Phys. Rev. E **67**, 036109 (2003).
[41] P. Jung and P. Hänggi, Phys. Rev. A **44**, 8032 (1991).
[42] F. Cooper, A. Khare, and U. Sukhatme, Phys. Rep. **251**, 267 (1995).
[43] H. Kalka and G. Soff, *Supersymmetrie* (Teubner, Stuttgart, 1997), in German.
[44] P. Jung and P. Hänggi, Europhys. Lett. **8**, 505 (1989).
[45] L. Callenbach, P. Hänggi, S. Linz, J. Freund, and L. Schimansky-Geier, Phys. Rev. E **65**, 051110 (2002).
[46] R. Benzi, A. Sutera, and A. Vulpiani, J. Phys. A **14**, L453 (1981).
[47] R. Benzi, G. Parisi, A. Sutera, and A. Vulpiani, Tellus **34**, 90 (1982).
[48] P. Jung and G. Mayer-Kress, Phys. Rev. Lett. **74**, 2130 (1995).
[49] F. Marchesoni, L. Gammaitoni, and A. R. Bulsara, Phys. Rev. Lett. **76**, 2609 (1996).
[50] M. Locher, G. A. Johnson, and E. R. Hunt, Phys. Rev. Lett. **77**, 4698 (1996).
[51] J. M. G. Vilar and J. M. Rubi, Phys. Rev. Lett. **78**, 2886 (1997).
[52] U. Siewert and L. Schimansky-Geier, Phys. Rev. E **58**, 2083 (1998).